Journal of Materials Chemistry C

PAPER

Polyurethane Derivatives for Highly Sensitive and Selective Fluorescent Detection of 2,4,6-Trinitrophenol (TNP)

Received 00th January 20xx,
Accepted 00th January 20xx

DOI: 10.1039/x0xx00000x

www.rsc.org/

Nan Jiang,‡[a] Guangfu Li,‡[a] Weilong Che,[a] Dongxia Zhu,*[a] Zhongmin Su*[a] and Martin R. Bryce*[b]

A series of luminescent non-conjugated polyurethane derivatives (PUs) has been obtained in a facile way in high yields. The polymers show highly selective and sensitive detection of 2,4,6-trinitrophenol (TNP) (picric acid). The selectivity for TNP is accomplished via combined strong inner filter effect (IFE), Förster resonance energy transfer (FRET) and photoinduced electron transfer (PET). A convenient indicator paper for the visual detection of TNP has been constructed by immobilization of the polymer **PU1** on filter paper. The **PU1**-coated filter paper presents a rapid detection of TNP in water with the low concentration limit of 10^{-10} M, ~0.229 ag/cm^2. This is a simple, low-cost and highly efficient method for the detection of TNP.

Introduction

In the 21st century, an increased frequency of terrorist bomb attacks and the use of land-mines have seriously threatened the security of human society. Consequently, the detection of explosives by practically simple methods has become an issue of paramount importance.[1-3] In this context 2,4,6-trinitrophenol (TNP) (picric acid) is an extremely dangerous substance that exhibits enhanced explosive power compared to the other nitro-aromatic compounds,[4] such as 2-nitrotoluene (oNT), nitrobenzene (NB) and 2,4,6-trinitrotoluene (TNT). TNP is also used in the dye industry and as a clinical chemistry reagent which can result in significant pollution of irrigation land and ground water supplies, with harmful effects to human health.[5,6] Therefore, the rapid and highly selective detection of TNP is needed. Among the various explosive detection techniques, such as gas chromatography mass spectroscopy (GC-MS),[7] surface enhanced Raman spectroscopy (SERS)[8] and electrochemical methods,[9] fluorescence sensing offers several advantages, such as high sensitivity, simplicity, rapid response time and low cost.[10-14] Some fluorescent chemosensors including MOFs,[15-17] quantum dots (QDs),[18,19] fluorescent polymers,[20-22] phosphorescent metal complexes,[23,24] and small molecule-based sensors[25,26] have been developed to detect nitro-aromatics. However, highly selective sensing of TNP compared with other nitro-aromatic explosives still remains a challenge, as they usually exhibit similar electron affinity.[27]

Polyurethanes (PUs) are a very versatile class of non-conjugated polymers with tuneable properties. They have found broad applications in everyday life as components of shape-memory materials, building insulation, furniture, clothing and fabrics.[28-30] However, due to a lack of extended π-conjugated chromophore units in the polymer chains, their luminescent properties and further optoelectronic applications have been mostly overlooked.[31-33] Recently, we reported a series of polyurethanes with unique low temperature long persistent luminescence.[34] The formation of carbonyl clusters from electron rich oxygen atoms in the polymer chains has been shown to be favourable for emission. Compared with traditional organic luminescent materials, non-conjugated PUs offer advantages in terms of facile chemical preparation, environment-friendliness, large-scale production and low cost.[28]

As a motivation for the present work we proposed that photoinduced electron transfer (PET) might occur between electron-rich polyurethanes and electron-deficient nitro-aromatic compounds, acting as electron donor and acceptor moieties, respectively. Thus, the sensing of explosives by fluorescence quenching could potentially be achieved by readily-accessible non-conjugated polyurethanes.

To test our hypothesis, a series of luminescent non-conjugated polyurethanes **PU1**–**PU3** has been rationally designed by incorporation of classical π-aromatic chromophores which give PUs good emission properties. The role of the carboxyl group in **PU1** is to increase the water solubility of **PU1** and further enhance the sensing efficiency for the nitro-aromatic compounds in water. All the PUs show highly selective and sensitive response for the turn-off fluorescent detection of TNP in both solution and solid states. The sensing can be rapidly recognized by naked eyes. The sensing mechanism can be attributed to a combination of inner

[a] Key Laboratory of Nanobiosensing and Nanobioanalysis at Universities of Jilin Province, Department of Chemistry, Northeast Normal University, 5268 Renmin Street, Changchun, Jilin Province 130024, P.R. China.
E-mail: zhudx047@nenu.edu.cn; zmsu@nenu.edu.cn
[b] Department of Chemistry, Durham University, Durham, DH1 3LE, UK.
E-mail: m.r.bryce@durham.ac.uk

† Electronic Supplementary Information (ESI) available: Experimental details, ^{1}H NMR spectra and photophysical properties. See DOI: 10.1039/x0xx00000x

‡ These authors contributed equally to the preparation of this work.

filter effect (IFE), Förster resonance energy transfer (FRET) and photoinduced electron transfer (PET) processes.

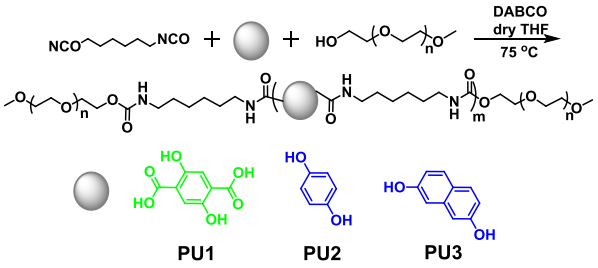

Scheme 1 Synthetic routes for **PU1**, **PU2** and **PU3**.

Results and discussion

The PU derivatives were synthesized by a facile procedure in high yield (Scheme 1) by analogy with previous analogues.[34] The chemical structures of the PUs were characterized by ^{1}H NMR spectroscopy and FTIR spectrometry. Details are given in the ESI. **PU1**, **PU2** and **PU3** possess good solubility in acetonitrile-water mixture (1:1 v/v) with intense green or blue emission. The corresponding photoluminescence quantum yields are 82%, 24% and 33%, respectively. The higher PLQY of **PU1** can be attributed to the intrinstic green emission of **PU1**. Green emitters usually show higher radiative transition constants when compared with the blue-emitters, such as **PU2** and **PU3**. The fluorescence sensing of explosives was studied by detailed photophysical investigations. Acetonitrile-water mixtures (1:1 v/v) were used for these investigations to guarantee that the PUs are fully dissolved and show intense emission. As shown in Fig. 1a, **PU1** exhibits intense emission with a peak at 527 nm in acetonitrile-water solution (1:1 v/v) (10 μM). A rapid and clearly visible fluorescence turn-off response was observed upon increasing the concentration of TNP in the solution. This enables the effective "real-time" detection of TNP. The emission quenching is clearly seen when 5 μM of TNP is added to the mixture; 91% of the emission is quenched when the concentration of TNP reached 30 μM. Similarly, the emission of **PU2** and **PU3** are also quenched by TNP in acetonitrile-water solutions (1:1 v/v) (10 μM), with quenching efficiencies of 96% and 99%, respectively. As shown in Fig. 1b, a Stern–Volmer (S–V) plot exhibited a hyperbolic curve with a straight line at lower concentration of TNP (up to 10 μM) and a S–V quenching constant of 1.22×10^5 M^{-1}. At higher concentration of TNP the shape of the curve is due to a superamplified quenching effect.[35] The non-linear behaviour of the S–V plot for TNP and the decreased fluorescence lifetime upon the addition of TNP (Fig. 1b insert), suggests that static and dynamic quenching processes coexist simultaneously during the detection.[36] The S–V curves for **PU2** and **PU3** are also nonlinear, and the quenching constants are 1.65×10^5 M^{-1} and 2.77×10^5 M^{-1}, respectively (Fig. S5 and S6, ESI†). These values are relatively high among the reported polymer and macromolecular sensors.[37-40] The limits of detection (LOD) for **PU1**–**PU3** as sensors for TNP are calculated to be 0.90, 1.01 and 0.57 μM, respectively, indicating a high sensitivity towards TNP.

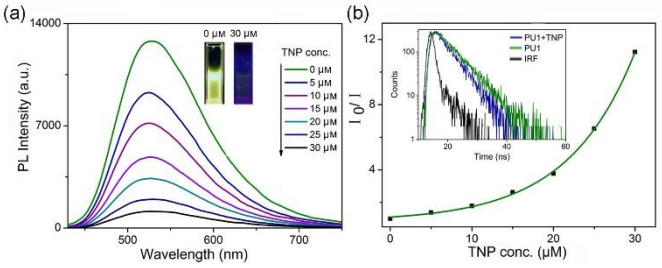

Fig. 1 (a) PL spectra of **PU1** (10 μM) in acetonitrile–water (v/v = 1 : 1) containing different amounts of trinitrophenol (TNP). Insert: Photographs of **PU1** (10 μM) before and after addition of TNP (30 μM). (b) Corresponding Stern–Volmer plot of TNP. Insert: the lifetime decay of **PU1** (10 μM) before and after addition of TNP (30 μM).

The emission response of PUs to other nitro-aromatic derivatives, such as nitrobenzene (NB), 3-nitrotoluene (mNT), 2,4-dinitrotoluene (2,4-DNT), p-nitrotoluene (NT), dinitrobenzene (DNB), 2,4,6-trinitrotoluene (TNT), 2,6-dinitrotoluene (2,6-DNT) and 2-nitrotoluene (oNT) were also studied. As shown in Fig. 2a, these nitro-aromatics had little effect on the emission intensity compared with that of TNP under the same conditions. Remarkably, for **PU1**, the fluorescence was significantly quenched when TNP (30 μM) was added into the **PU1** solutions containing the other nitro-aromatic species (Fig. 2b). Similar results were also observed for **PU2** and **PU3** (Fig. S7, ESI†). These results clearly indicate the unprecedented selectivity of PUs for TNP.

To understand the origin of the selectivity of PUs towards TNP, the sensing mechanism was investigated. As previously mentioned, the non-linear behaviour of the S–V plot for TNP implies a resonance energy transfer mechanism in the quenching process, suggesting the possibility of simultaneous static and dynamic quenching.[36] The fluorescence lifetime of **PU1** (10 μM) decreased from 5.58 ns to 4.45 ns upon the addition of TNP (30 μM) (Fig. 1b insert), which is consistent with the involvement of a dynamic quenching process.[16]

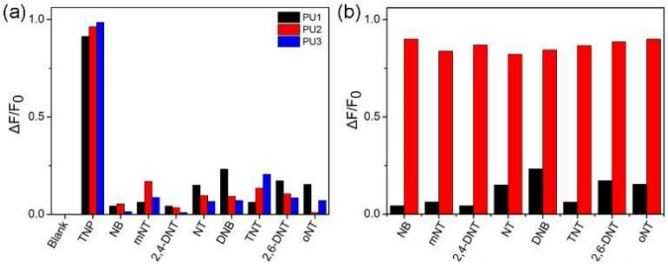

Fig. 2 (a) Quenching efficiency of PUs upon addition of different analytes (30 μM) in acetonitrile-water (1:1 v/v) (10 μM) solution. (b) Quenching efficiency of **PU1** (10 μM) with analytes (30 μM) in acetonitrile-water (1:1 v/v) mixtures before (black) and after (red) the addition of TNP (30 μM). $\Delta F = F_0 - F$, where F_0 and F denote the fluorescence intensity of PUs before and after the addition of

analytes, respectively.

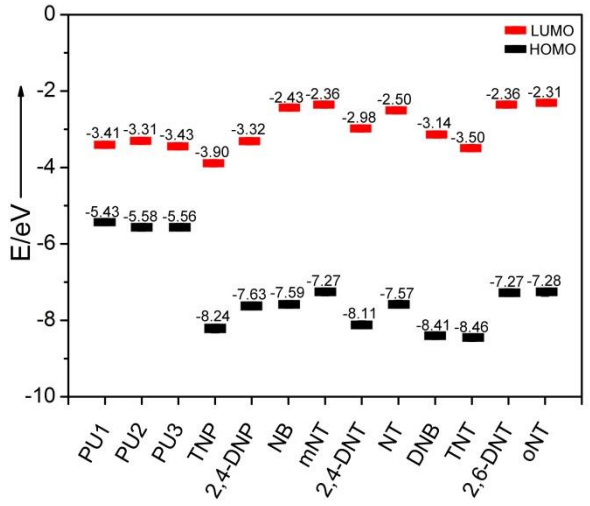

Fig. 3 HOMO and LUMO energy levels for the PUs and nitro-aromatic derivatives.

To assess the feasibility of photoinduced electron transfer from electron-rich PUs to the electron-deficient nitro-aromatics[35] the energy levels of the highest occupied molecular orbital (HOMO) and lowest occupied molecular orbital (LUMO) of the PUs were measured by cyclic voltammetry (CV). As shown in Fig. 3, the higher LUMO energy of the PUs would be expected to facilitate the electron transfer to the lower lying LUMOs of the analytes, making PET a possible mechanism for quenching of the PUs' fluorescence in response to analytes. It is worth noting that electron transfer may also occur from the PUs to TNT. However, the negligible quenching efficiency for TNT (Fig. 2a) indicates that PET is not the only reason for the highly selective fluorescence quenching for TNP.

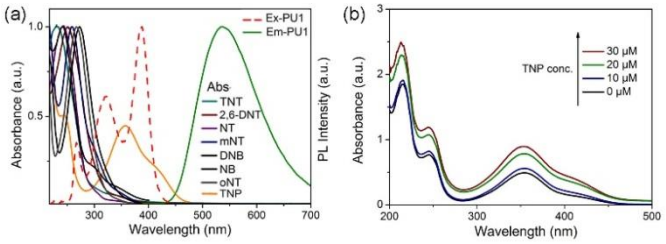

Fig. 4 (a) Normalized absorption spectra of nitro-aromatics and excitation/emission spectra of **PU1**. (b) UV-visible spectra of **PU1** (1×10^{-5} M) upon addition of different amounts of TNP.

It is well known that Förster resonance energy transfer can occur when the emission band of a probe overlaps with the absorption band of an analyte.[36] As observed in Fig. 4a, there is overlap between the absorption spectrum of TNP and the emission spectrum of **PU1**, while essentially no overlap is seen for the other nitro-aromatic analytes. This implies that FRET may be involved in the quenching process with sufficient energy transfer in the case of TNP to amplify the quenching efficiency, resulting in the enhanced detection selectivity as well as sensitivity. To verify this assumption, the overlap between the absorption band of the analytes and the emission spectra of **PU2** and **PU3** are shown in Fig. S8 and S9 (ESI†), respectively. It can be seen that the extent of overlap is in the sequence **PU3** > **PU2** > **PU1**, which explains why the sensitivity to TNP follows that same sequence (Fig. 2a).

Recently, the inner filter effect (IFE) has gained much attention in the field of enhanced fluorescence quenching for turn-off sensors, for example in the detection of TNP by a conjugated polyfluorene derivative substituted with pendant amino groups.[41] IFE is a different phenomenon from ground-state charge-transfer and FRET: for an IFE sensing system the absorption spectrum of the analyte should possess a substantial spectral overlap with the excitation and/or emission spectrum of the fluorescent molecule.[42] For TNP, the wide overlap between the excitation/emission spectra of **PU1** and absorption spectra of TNP reveals that IFE may exist in the quenching system (Fig. 4a). The UV−visible absorption spectra of **PU1** showed a gradual increase in the absorption intensity with an increase of TNP concentration, without causing any shift in the peak of **PU1** (Fig. 4b). Similar results were also observed for **PU2** and **PU3** (Fig. S10, ESI†). This excludes the possibility of the formation of a ground-state charge transfer complex between PUs and TNP.[41] Moreover, negligible overlap between the exciton/emission spectra of PUs and the absorption spectra of other nitro-aromatics (Fig. 4a, S8 and S9) indicates no IFE in these systems. Therefore, all the data suggest that combined FRET and IFE is predominantly responsible for the high selectivity and sensitivity of PUs towards TNP.

^{1}H NMR spectra for **PU1** demonstrated most of the proton signals of **PU1** showed no observable change upon the addition of TNP to DMSO-d_6 (Fig. S11, ESI†). Only the proton of the pendant carboxyl group shifted, probably due to H-bonding of the strongly acidic OH group of TNP. These results indicate that the PUs retain their backbone structure in the presence of TNP. The possibility of formation of a ground-state complex in the quenching process can also be excluded (Fig. S13 and S14, ESI†).

To further investigate the role of an electrostatic complex on quenching efficiency, TNP, 2,4-DNP and NP, all containing a single −OH group with a variable number of $-NO_2$ groups, were studied. TNP is a stronger acid compared to 2,4-DNP and 4-NP, and therefore has a greater tendency to interact with PUs via acid−base interaction to form a stable electrostatic complex.[43] The fluorescence quenching efficiency of **PU1** was found to be in the order TNP > 2,4-DNP > 4-NP (Fig. S15, ESI†). The similar spectral overlap between the excitation/emission spectra of **PU1** and absorption spectra of TNP, 2,4-DNP and 4-NP indicates that a FRET process is not the main explanation for the quenching efficiency decreasing from TNP to NP (Fig. S16, ESI†). PET from **PU1** to TNP induced by acid−base interaction reasonably explains the higher quenching efficiency among TNP, 2,4-DNP and NP.

To demonstrate a proof-of-concept practical application of PUs for the detection of TNP, polymer-coated indicator paper was constructed by simply immersing standard filter paper in an acetonitrile-water solution of **PU1**, and then drying the paper at room temperature in air. As shown in Fig. 5, under 365 nm UV

illumination, the paper showed intense green fluorescence from the original emission of **PU1**. It can be seen clearly that the intense fluorescence is quenched rapidly and sensitively by adding a drop of TNP (30 μM) in pure water solution onto the paper. However, no fluorescence quenching was observed when other nitro-aromatic compounds were added onto the paper (Fig. 5A). To study the sensitivity for the detection of TNP, different concentrations of TNP water solutions (10 μL) were poured over the 1 cm^2 **PU1**-coated filter paper (Fig. 5B). The fluorescent quenching efficiency of **PU1** obviously increased with increasing the concentration of TNP. The visible limit of detection (LOD) for TNP in water solutions is remarkably low at 10^{-10} M, ~0.229 ag/cm^2. The visible LOD of **PU2** and **PU3**-coated filter papers for TNP is 10^{-3} M (Fig. S17). The lower LOD of **PU2** and **PU3** for TNP can be attributed to their less efficient blue emission when compared with highly efficient green-emissive **PU1**. Therefore, the as-prepared PUs, especially **PU1**, exhibit great potential for the rapid, sensitive and selective detection of TNP.

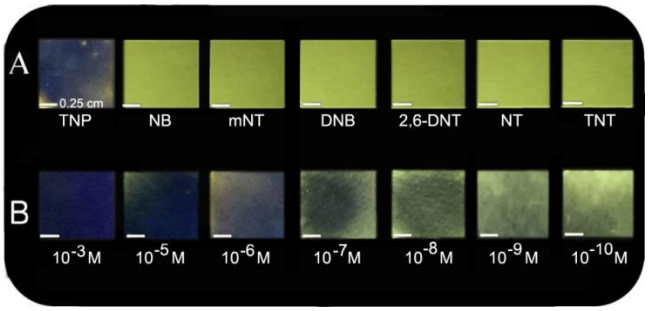

Fig. 5 (A) Luminescent photographs of **PU1**-coated filter paper with addition of different nitro-aromatic compounds (30 μM) on contact mode with a spot area of ~1 cm^2. (B) Photograph of the fluorescence quenching of **PU1**-coated filter paper with different concentrations of TNP (10 μL) water solutions. All photographs were taken under 365 nm UV illumination.

Conclusions

In conclusion, a series of luminescent non-conjugated polyurethane derivatives has been designed and synthesized in a facile way with high yields, and they exhibit highly sensitive and selective detection of TNP. The sensing mechanism can be attributed to the combined strong inner filter effect (IFE), Förster resonance energy transfer (FRET) and photoinduced electron transfer (PET). IFE and FRET should be predominantly responsible for the high selectivity and sensitivity of PUs towards TNP. PET also plays a role for the quenching when we investigate the role of electrostatic complex formation on the quenching efficiency. Furthermore, an indicator paper for the visual detection of TNP has been constructed by immobilization of **PU1** on filter paper. **PU1**-coated filter paper presents rapid monitoring of TNP with a remarkably low detection limit of 10^{-10} M, ~0.229 ag/cm^2. This study paves a convenient way towards the development of sensing hazardous TNP using low-cost non-conjugated polyurethane materials.

Conflicts of interest

There are no conflicts to declare.

Acknowledgements

The work was funded by NSFC (No.51473028), the key scientific and technological project of Jilin province (20150204011GX, 20160307016GX), the Development and Reform Commission of Jilin province (20160058). M. R. B. thanks EPSRC grant EP/K039423/1 for funding.

Notes and references

1 E. B. Ford, V. Lystad and F. A. Rasio, *Nature*, 2005, **434**, 873–876.
2 A. Lichtenstein, E. Havivi, R. Shacham, E. Hahamy, R. Leibovich, A. Pevzner, V. Krivitsky, G. Davivi, I. Presman, R. Elnathan, Y. Engel, E. Flaxer and F. Patolsky, *Nat. Commun.*, 2014, **5**, 4195.
3 M. H. Wong, J. P. Giraldo, S. Y. Kwak, V. B. Koman, R. Sinclair, T. T. Lew, G. Bisker, P. Liu and M. S. Strano, *Nat. Mater.*, 2017, **16**, 264–272.
4 B. Wang, Y. Mu, C. Zhang and J. Li, *Sens. Actuators B: Chem.*, 2017, **253**, 911–917.
5 J. F. Xiong, J. X. Li, G. Z. Mo, J. P. Huo, J. Y. Liu, X. Y. Chen and Z. Y. Wang, *J. Org. Chem.*, 2014, **79**, 11619–11630.
6 B. Ju, Y. Wang, Y. M. Zhang, T. Zhang, Z. Liu, M. Li and S. Xiao-An Zhang, *ACS Appl. Mater. Interfaces*, 2018, **10**, 13040–13047.
7 K. M. Roscioli, E. Davis, W. F. Siems, A. Mariano, W. Su, S. K. Guharay and H. H. Hill, Jr., *Anal. Chem.*, 2011, **83**, 5965–5971.
8 J. M. Sylvia, J. A. Janni, J. D. Klein and K. M. Spencer, *Anal. Chem.*, 2000, **72**, 5834–5840.
9 E. S. Forzani, D. Lu, M. J. Leright, A. D. Aguilar, F. Tsow, R. A. Lglesias, Q. Zhang, J. Lu, J. Li and N. Tao, *J. Am. Chem. Soc.*, 2009, **131**, 1390–1391.
10 P. Das and S. K. Mandal, *J. Mater. Chem. C*, 2018, **6**, 3288-3297.
11 S. S. R. Dasary, A. K. Singh, K. S. Lee, H. Yu and P. C. Ray, *Sens. Actuators B: Chem.*, 2018, **255**, 1646–1654.
12 H. Ma, F. Li, L. Yao, Y. Feng, Z. Zhang and M. Zhang, *Sens. Actuators B: Chem.*, 2018, **259**, 380–386.
13 H. Turhan, E. Tukenmez, B. Karagoz and N. Bicak, *Talanta*, 2018, **179**, 107–114.
14 Y. Salinas, R. Martínez-Manez, M. D. Marcos, F. Sancenon, A. M. Costero, M. Parra, S. Gil, *Chem. Soc. Rev.*, 2012, **41,** 1261−1296.
15 D. M. Chen, N. N. Zhang, C. S. Liu and M. Du, *ACS Appl. Mater. Interfaces*, 2017, **9**, 24671–24677.
16 X.-G. Liu, C.-L. Tao, H.-Q. Yu, B. Chen, Z. Liu, G.-P. Zhu, Z. Zhao, L. Shen and B. Z. Tang, *J. Mater. Chem. C*, 2018, **6**, 2983–2988.
17 C. F. Pereira, F. Figueira, R. F. Mendes, J. Rocha, J. T. Hupp, O. K. Farha, M. M. Q. Simoes, J. P. C. Tome and F. A. A. Paz, *Inorg. Chem.*, 2018, **57**, 3855–3864.
18 F. Cheng, X. An, C. Zheng and S. Cao, *RSC Advances*, 2015, **5**, 93360–93363.

19 D. Peng, L. Zhang, F. F. Li, W. R. Cui, R. P. Liang and J. D. Qiu, *ACS Appl. Mater. Interfaces*, 2018, **10**, 7315–7323.
20 S. Shanmugaraju, D. Umadevi, A. J. Savyasachi, K. Byrne, M. Ruether, W. Schmitt, G. W. Watson and T. Gunnlaugsson, *J. Mater. Chem. A*, 2017, **5**, 25014–25024.
21 Y. Zhang, P. Shen, B. He, W. Luo, Z. Zhao and B. Z. Tang, *Polym. Chem.*, 2018, **9**, 558–564.
22 Y. W. Wu, A. J. Qin and B. Z. Tang, *Chinese J. Polym. Sci.*, 2017, **35**, 141–154.
23 L. L.Wen, X. G. Hou, G. G. Shan, W. L. Song, S. R. Zhang, H. Z. Sun and Z. M. Su, *J. Mater. Chem. C*, 2017, **5**, 10847–10854.
24 W. L. Che, G. F. Li, X. M. Liu, K. Z. Shao, D. X. Zhu, Z. M. Su and M. R. Bryce, *Chem. Commun*., 2018, **54**, 1730–1733.
25 Y. Peng, A. J. Zhang, M. Dong and Y. W. Wang, *Chem. Commun*., 2011, **47**, 4505–4507.
26 Y. Xu, B. Li, W. Li, J. Zhao, S. Sun and Y. Pang, *Chem. Commun*., 2013, **49**, 4764–4766.
27 B. Xu, X. Wu, H. Li, H. Tong and L. Wang, *Macromolecules*, 2011, **44**, 5089–5092.
28 A. Lendlein and S. Kelch, *Angew. Chem. Int. Ed*., 2002, **41**, 2034–2057
29 D. K. Chattopadhyay and K. V. S. N. Raju, *Prog. Polym. Sci.*, 2007, **32**, 352–418.
30 C. Liu, H. Qin and P. T. Mather, *J. Mater. Chem.*, 2007, **17**, 1543–1558.
31 Y. Q. Niu, T. He, J. Song, S. P. Chen, X. Y. Liu, Z. G. Chen, Y. J. Yu and S. G. Chen, *Chem. Commun*., 2017, **53**, 7541–7544.
32 W. Sun, Z. Wang, T. Wang, L. Yang, J. Jiang, X. Zhang, Y. Luo and G. Zhang, *J. Phys. Chem. A*, 2017, **121**, 4225–4232.
33 Y. Wu, J. Hu, H. Huang, J. Li, Y. Zhu, B. Tang, J. Han and L. Li, *J. Polym. Sci. Part B: Polym. Phys.*, 2014, **52**, 104–110.
34 N. Jiang, G.-F. Li, B.-H. Zhang, D.-X. Zhu, Z.-M. Su and M. R. Bryce, *Macromolecules*, 2018, **51**, 4178–4184.
35 J. Liu, Y. Zhong, P. Lu, Y. Hong, J. W. Y. Lam, M. Faisal, Y. Yu, K. S. Won and B. Z. Tang, *Polym. Chem*., 2010, **1**, 426–429.
36 X. G. Hou, Y. Wu, H. T. Cao, H. Z. Sun, H. B. Li, G. G. Shan and Z. M. Su, *Chem. Commun.*, 2014, **50**, 6031–6034.
37 J. Wang, J. Mei, W. Z. Yuan, P. Lu, A. J. Qin, J. Z. Sun, Y. G. Ma and B. Z. Tang, *J. Mater. Chem.*, 2011, **21,** 4056–4059.
38 S. Joshi, S. Kumari, E. Chamorro, D. D. Pant and R. Sakhuja, *ChemistrySelect*, 2016, **1**, 1756–1762.
39 A. H. Malik and P. K. Iyer, *ACS Appl. Mater. Interfaces*, 2017, **9,** 4433–4439.
40 H. Arora, S. Pramanik, M. Kumar and V. Bhalla, *New J. Chem.*, 2016, **40,** 3187–3193.
41 A. S. Tanwar, S. Hussain, A. H. Malik, M. A. Afroz and P. K. Iyer, *ACS Sensors*, 2016, **1**, 1070–1077.
42 S. Chen, Y-L. Yu, J-H. Wang, *Analytica Chimica Acta*, 2018, **999,** 13-26.
43 K. Bauri, B. Saha, J. Mahanti and P. De, *Polym. Chem*., 2017, **8**, 7180–7187.

Supporting Information

Polyurethane Derivatives for Highly Sensitive and Selective Fluorescent Detection of 2,4,6-Trinitrophenol (TNP)

Nan Jiang,‡[a] Guangfu Li,‡[a] Weilong Che,[a] Dongxia Zhu,*[a] Zhongmin Su*[a] and Martin R. Bryce*[b]

[a] Key Laboratory of Nanobiosensing and Nanobioanalysis at Universities of Jilin Province, Department of Chemistry, Northeast Normal University, 5268 Renmin Street, Changchun, Jilin Province 130024, P. R. China
[b] Department of Chemistry, Durham University, Durham, DH1 3LE, UK
E-mail: m.r.bryce@durham.ac.uk

Table of Contents: **Page**

1. Experimental details

General

Materials obtained from commercial suppliers were used without further purification unless otherwise stated. All glassware, syringes, magnetic stirring bars, and needles were thoroughly dried in a convection oven. ^{1}H NMR spectra were recorded at 25 ºC on a Varian 500 MHz spectrometer and were referenced internally to the residual proton resonance in DMSO-d_6 (δ 2.5 ppm). The molecular weights of the polymers were calculated from their ^{1}H NMR spectra. UV-vis absorption spectra were recorded on a Shimadzu UV-3100 spectrophotometer. Photoluminescence spectra were collected on an Edinburgh FLS920 spectrophotometer.

Synthesis of PU Derivatives

PU1. A mixture of 2,5-dihydroxyterephthalic acid (2.62 mmol), polyethylene glycol mono-methyl ether (M_w = 200 g mol^{-1}; 1.98 mmol), anhydrous THF (8 mL)， hexamethylene diisocyanate (3.61 mmol) and DABCO (0.105 mmol) were added to dried two-neck round-bottom flask. The solution was heated at 75°C for 8 h under nitrogen atmosphere. After the clear solution became significantly viscous, product precipitated from excess diethyl ether. Then the product was dried under vacuum for 24 h to obtain the resulting **PU1** Yield: 84.6%. ^{1}H NMR (500 MHz, DMSO-d_6, δ [ppm]): 12.41 (s, 2H), 7.01-7.95 (broad, 2H), 4.02 (s, 4H), 3.36-3.69 (broad, PEG protons), 3.23 (s, 6H; PEG terminal -OCH_3 protons), 2.63-2.98 (broad, 4H), 1.45 (broad, 4H), 1.29 (broad, 4H). FTIR: 3323 cm^{-1}(N-H), 2859 and 2941cm^{-1}(-CH_2- asymmetric and symmetric stretch), 1704 (C=O), 1193 cm^{-1} (C-O-C stretch PEG). The molecular weight is 716 g mol^{-1} calculated from the ^{1}H NMR spectra.

PU2. The synthetic procedure for **PU2** was the same as **PU1**, except monomer hydroquinone (2.62 mmol) was used instead of 2,5-dihydroxyterephthalic acid. Yield: 83%. ^{1}H NMR (500 MHz, DMSO-d_6, δ [ppm]): 7.04-7.21 (broad, 4H ;), 4.03 (s, 4H), 3.39-3.61 (broad, PEG protons), 3.23 (s, 6H; PEG terminal -OCH_3 protons), 2.98 (broad, 4H), 1.41 (broad, 4H), 1.26 (broad, 4H). FTIR: 3326 cm^{-1}(N-H), 2859 and 2942 cm^{-1} (-CH_2- asymmetric and symmetric stretching), 1705 cm^{-1} (C=O), 1193 cm^{-1} (C-O-C stretching PEG). The molecular weight is 1077 g mol^{-1} calculated from the ^{1}H NMR spectra.

PU3. The synthetic procedure of **PU3** was the same as **PU1**, except monomer 2, 7-dihydroxynaphthalene (2.62 mmol) was used instead of 2,5-dihydroxyterephthalic acid.

Yield: 80.5%. ^{1}H NMR (500 MHz, DMSO-d_6, δ [ppm]): 7.04-7.95 (broad, 6H), 4.04 (broad, 4H), 3.45-3.62 (broad, PEG protons), 3.23 (s, 6H; PEG terminal -OCH_3- protons), 3.01 (s, 4H), 1.43 (s, 4H), 1.31 (s, 4H). FTIR: 3322 cm^{-1} (N-H), 2858 and 2940 cm^{-1} (-CH_2- asymmetric and symmetric stretching), 1704 cm^{-1} (C=O), 1191 cm^{-1} (C-O-C stretching PEG). The molecular weight is 3112 g mol^{-1} calculated from the ^{1}H NMR spectra.

Procedure for the sensing studies in the solution

Stock solutions of nitro-aromatic compounds, namely, picric acid (TNP), nitrobenzene (NB), 2,4-dinitrophenol (2,4-DNP) p-nitrophenol (NP), trinitrotoluene (TNT), 4-nitrotoluene (NT), 2,4-dinitrotoluene (2,4-DNT) and 2,6-dinitrotoluene (2,6-DNT) were prepared in acetonitrile-water mixture (1:1 v/v) at concentrations of 1×10^{-3} M, respectively. The absorption and fluorescence measurements of PUs (1×10^{-5} M) were carried out by sequentially adding different nitro-aromatic compounds in a quartz cuvette (3 cm × 3 cm). The absorption and fluorescence spectra of the resultant mixtures were then recorded after mixing thoroughly at room temperature.

Fluorescence quenching (%) measurement

The quenching percentage was calculated using the equation as follows:

Fluorescence quenching % = $(1 - I/I_0) \times 100\%$

where I_0 is the initial fluorescence intensity in the absence of analyte, I is the fluorescence intensity in the presence of corresponding analyte.

Fluorescence quenching titration study

The Stern–Volmer relationship establishes the correlation of intensity changes with the quencher concentration [Q] as follows:

$I_0/I = 1 + KSV\,[Q]$

where I_0 and I are the intensity, in the absence and presence of TNP, respectively, *KSV* is the Stern-Volmer quenching constant and [Q] is the concentration of TNP.

Benesi–Hildebrand equation

$1/(F_0 - F_i) = 1/\{Ka * (F_0\text{-}F_{Min}) * [PA]\} + 1/(F_0\text{-}F_{Min})$

where, F_0 is the fluorescence intensity of sensor, F_i is the fluorescence intensity obtained with TNP at different concentration, F_{Min} is the fluorescence intensity obtained with excess amount of TNP.

Lifetime measurements

$F(t) = \sum \alpha_i \exp(t / \tau_i)$

Where, α_i is a pre-exponential factor representing the fractional contribution to the time resolved decay of the component with a lifetime τ_i.

Method for detection limit calculation

The detection limit (LOD) was then calculated using the equation **3σ/K**, where σ is the standard deviation (SD) for PUs solution intensity in the absence of TNP and K denotes the slope of the curve.

2. Structural characterization of PUs

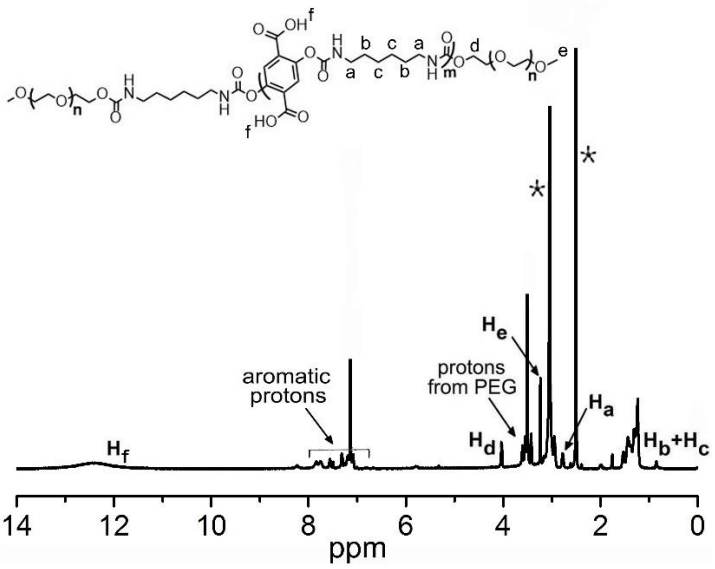

Fig. S1 ^{1}H NMR spectrum of **PU1** in DMSO-d_6 (* indicates peaks from the solvent and water)

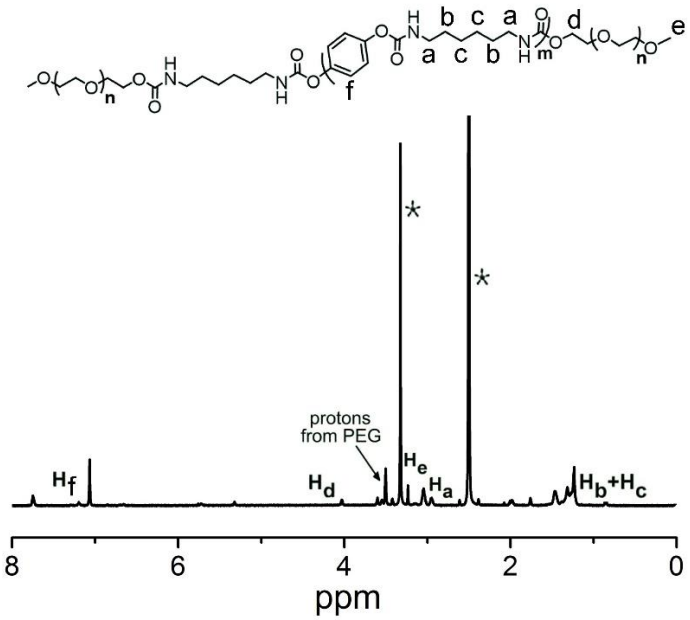

Fig. S2 ^{1}H NMR spectrum of **PU2** in DMSO-d_6 (* indicates peaks from the solvent and water)

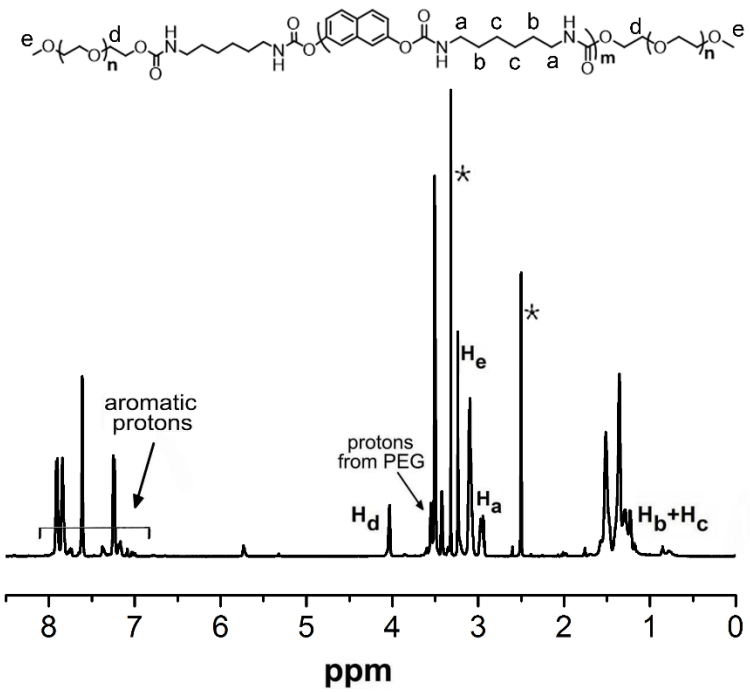

Fig. S3 ^{1}H NMR spectrum of **PU3** in DMSO-d_6 (* indicates peaks from the solvent and water).

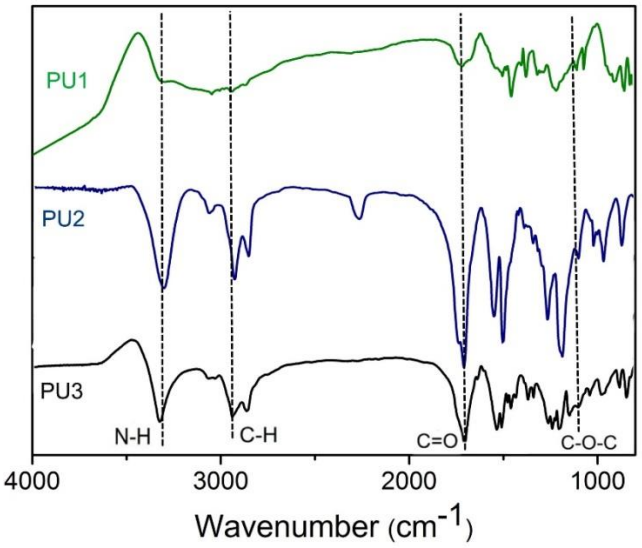

Fig. S4 FTIR spectra of **PU1**, **PU2** and **PU3**.

3. Photophysical properties and interactions of PUs with nitro-aromatic analytes

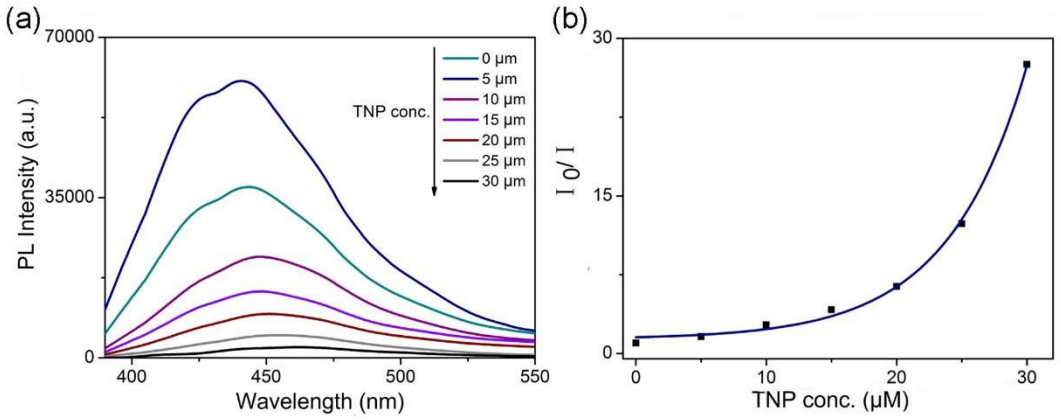

Fig. S5 (a) PL spectra of **PU2** (10 μM) in acetonitrile–water (v/v = 1:1) solution containing different amounts of TNP. (b) Corresponding Stern–Volmer plot of TNP.

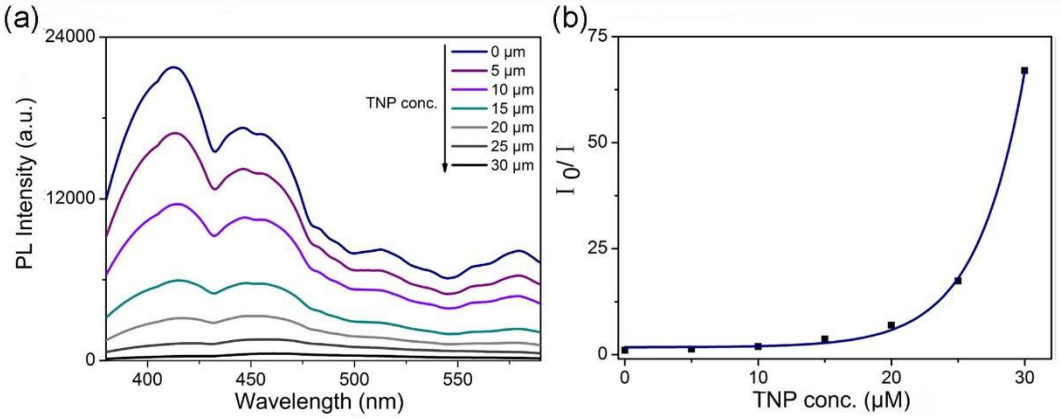

Fig. S6 (a) PL spectra of **PU3** (10 μM) in acetonitrile–water (v/v = 1:1) solution containing different amounts of TNP. (b) Corresponding Stern – Volmer plot of TNP.

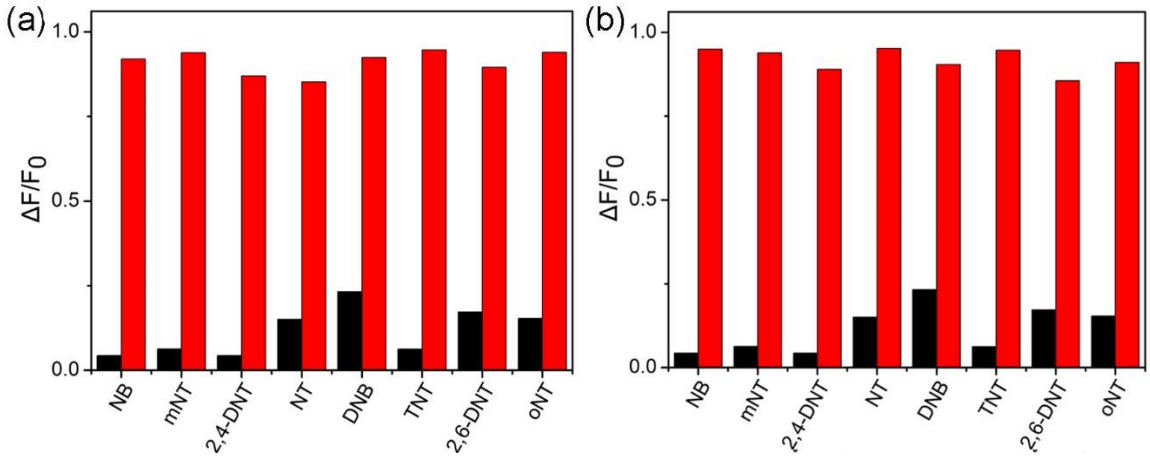

Fig. S7 (a) Quenching efficiency of **PU2** (10 μM) with analytes (30 μM) in acetonitrile-water (v/v = 1:1) solution before (black) and after (red) the addition of TNP (30 μM). (b) Quenching efficiency of **PU3** (10 μM) with analytes (30 μM) in acetonitrile-water (v/v = 1:1) solution before (black) and after (red) the addition of TNP (30 μM).

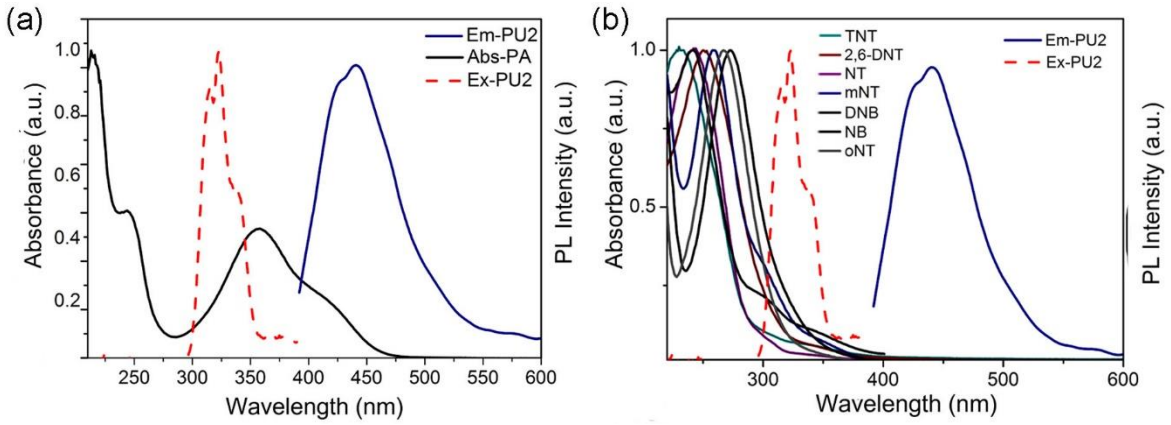

Fig. S8 (a) Normalized absorption spectrum of TNP and excitation/emission spectra of **PU2**. (b) Overlap between emission spectra of **PU2** and absorption spectra of various nitro-aromatics.

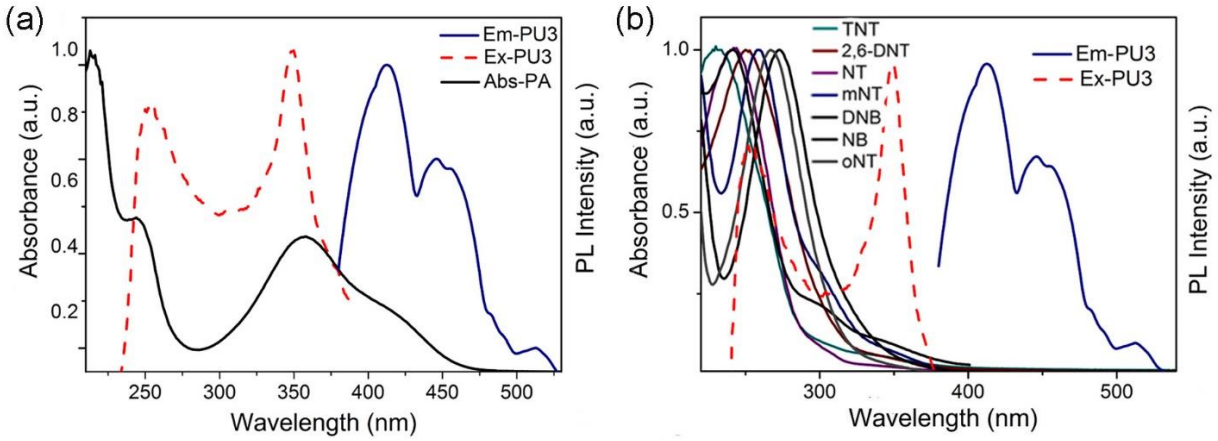

Fig. S9 (a) Normalized absorption spectrum of TNP and excitation/emission spectra of **PU3**. (b) Overlap between emission spectra of **PU3** and absorption spectra of various nitro-aromatics.

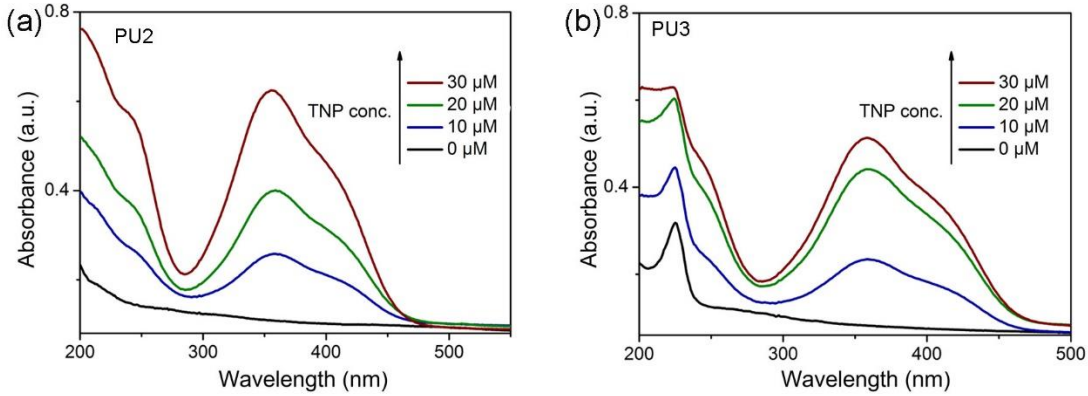

Fig. S10 UV-visible spectra of **PU2** (a) and **PU3** (b) (1×10^{-5} M) with increasing concentration of TNP.

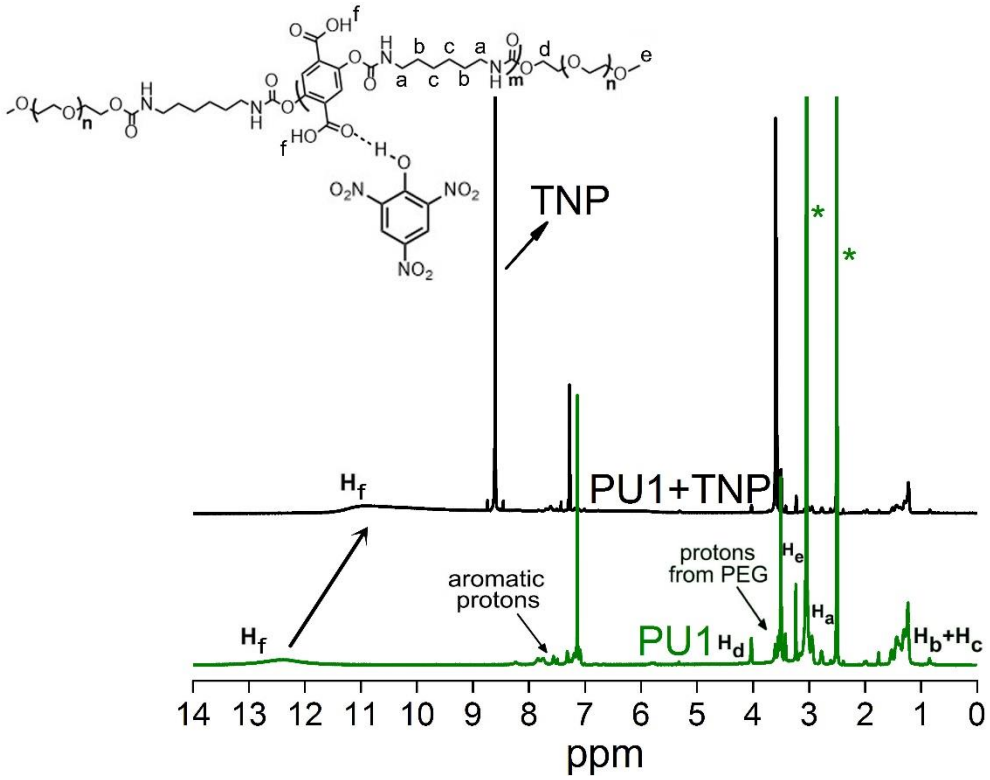

Fig. S11 ^{1}H NMR spectra of **PU1** before and after addition of 1 equivalent of TNP in DMSO-d_6.

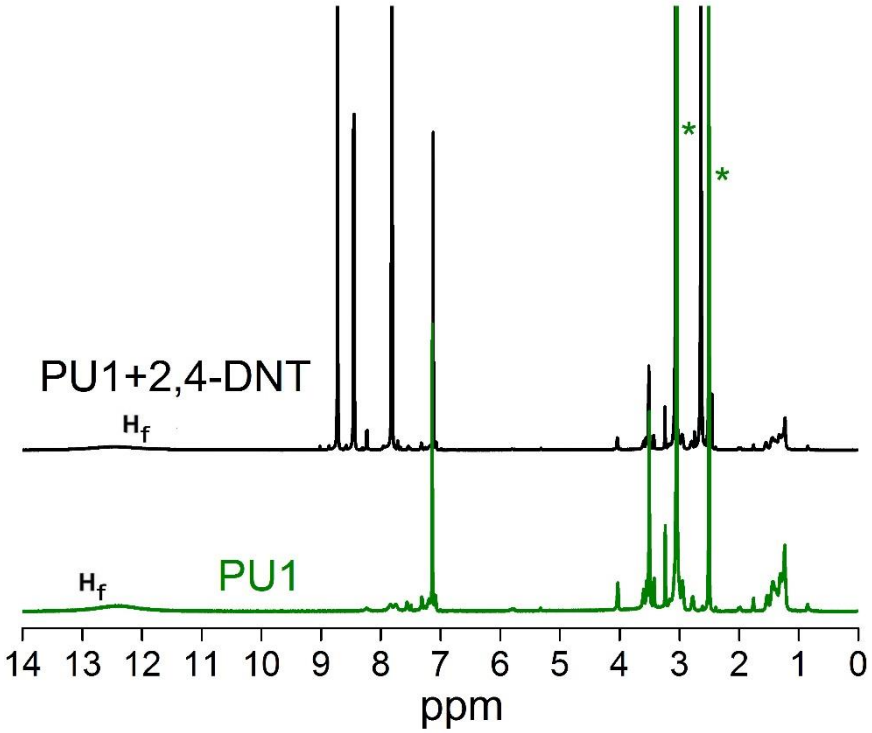

Fig. S12 ^{1}H NMR spectra of **PU1** before and after addition of 1 equivalent of 2,4-DNT in DMSO-d_6.

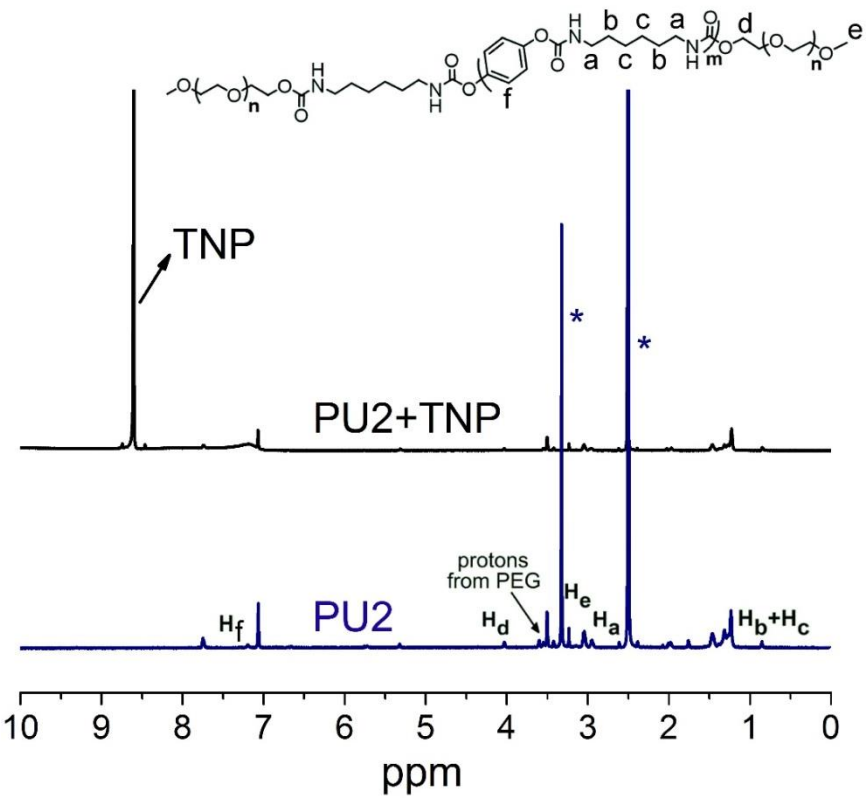

Fig. S13 ^{1}H NMR spectra of **PU2** before and after addition of 1 equivalent of 2,4-DNT in DMSO-d_6.

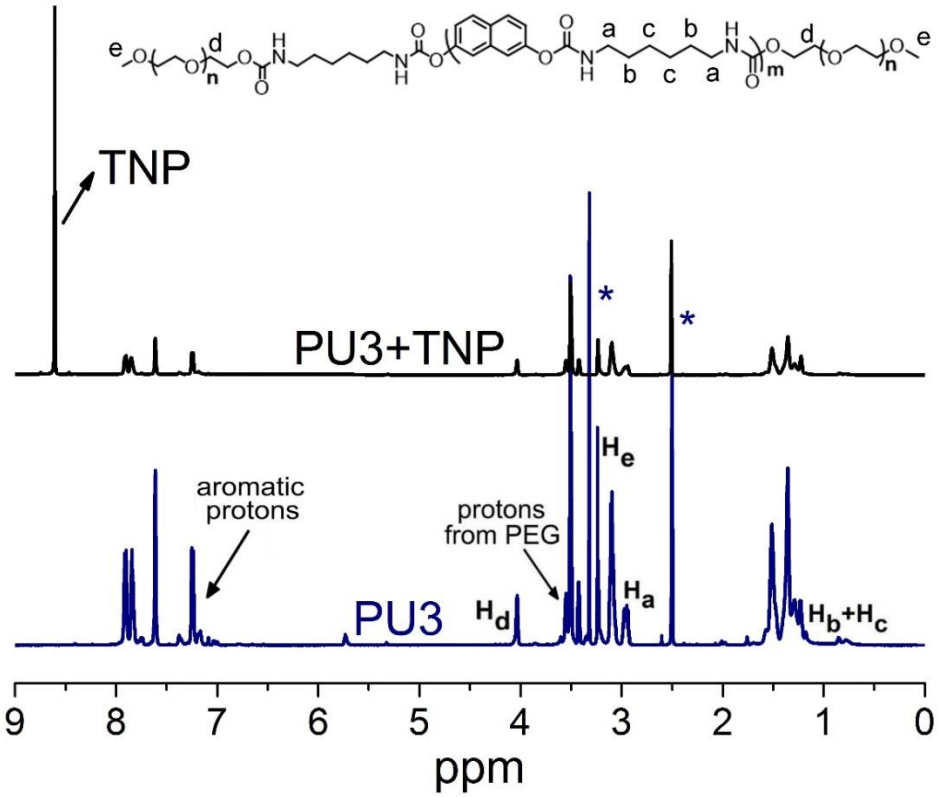

Fig. S14 ^{1}H NMR spectra of **PU3** before and after addition of 1 equivalent of 2,4-DNT in DMSO-d_6.

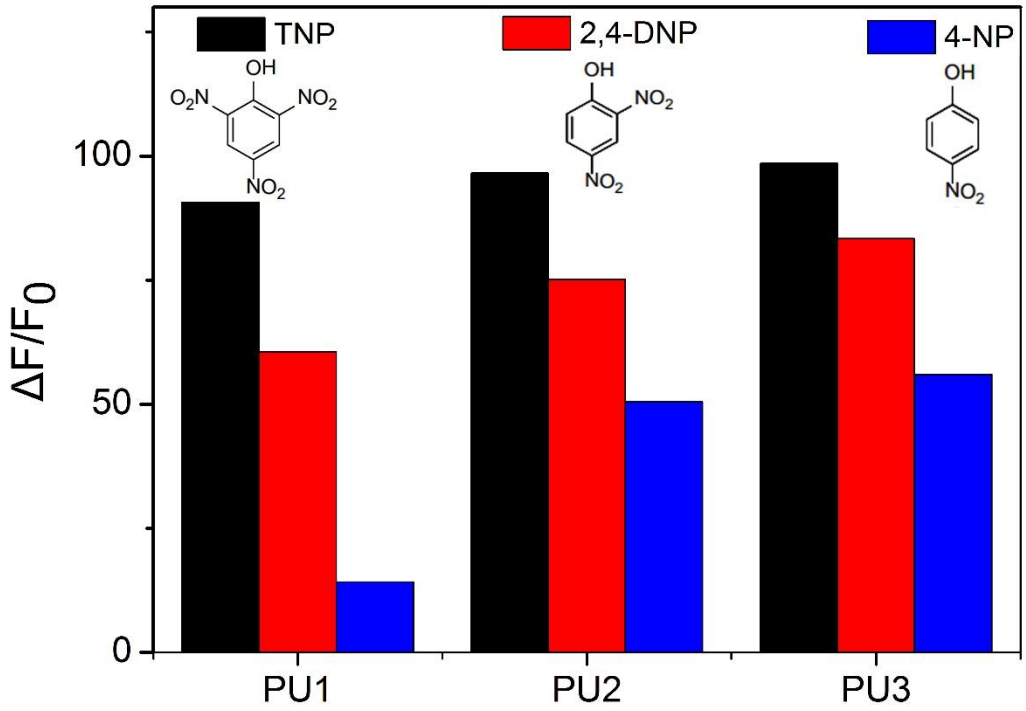

Fig. S15 Comparison of the fluorescence quenching of PUs caused by the addition of various nitrophenols (TNP, 2,4-DNP and 4-NP) (30 μM) in acetonitrile–water (v/v = 1:1) solution.

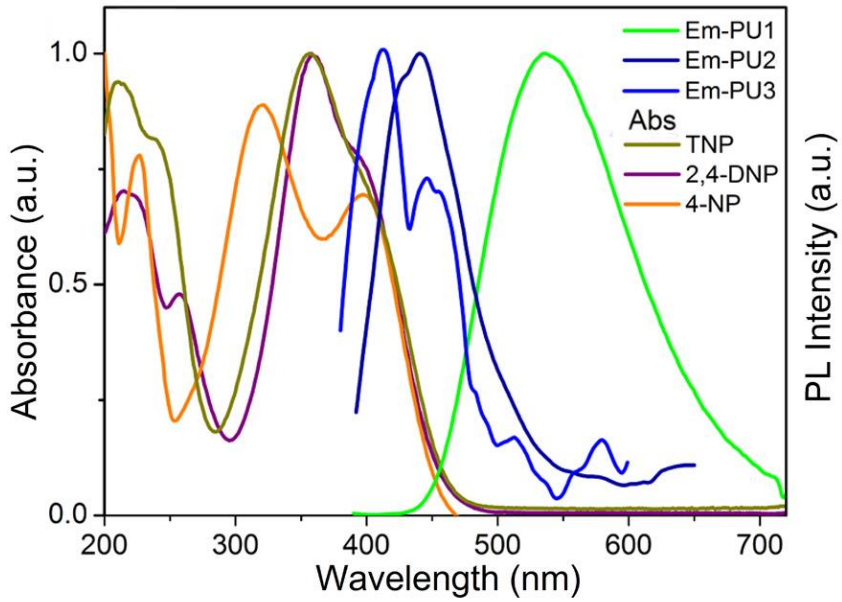

Fig. S16 Overlap between emission spectra of PUs and absorption spectra of various nitro-aromatics.

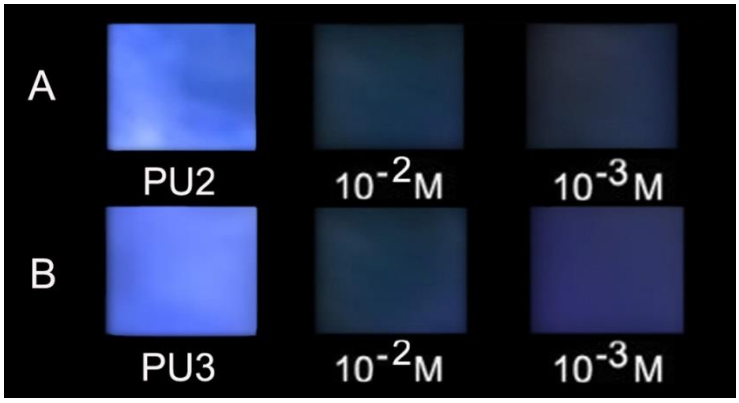

Fig. S17 (A) Luminescent photographs of **PU2**-coated filter paper with addition of different concentrations of TNP (10 μL) water solutions. (B) Luminescent photographs of **PU3**-coated filter paper with addition of different concentrations of TNP (10 μL) water solutions. All photographs were taken under 365 nm UV illumination.